Selective adsorption of block copolymers on patterned surfaces

Maria Sabaye Moghaddam[a] and Hue Sun Chan
Department of Biochemistry and Department of Medical Genetics and Microbiology, Faculty of Medicine, University of Toronto, Toronto, Ontario M5S 1A8, Canada

(Received 18 July 2006; accepted 11 September 2006; published online 27 October 2006)

Adsorption of copolymers on patterned surfaces is studied using lattice modeling and multiple Markov chain Monte Carlo methods. The copolymer is composed of alternating blocks of *A* and *B* monomers, and the adsorbing surface is composed of alternating square blocks containing *C* and *D* sites. Effects of interaction specificity on the adsorbed pattern of the copolymer and the sharpness of the adsorption transition are investigated by comparing three different models of copolymer-surface interactions. Analyses of the underlying energy distribution indicate that adsorption transitions in our models are not two-state-like. We show how the corresponding experimental question may be addressed by calorimetric measurements as have been applied to protein folding. Although the adsorption transitions are not "first order" or two-state-like, the sharpness of the transition increases when interaction specificity is enhanced by either including more attractive interaction types or by introducing repulsive interactions. Uniformity of the pattern of the adsorbed copolymer is also sensitive to the interaction scheme. Ramifications of the results from the present minimalist models of pattern recognition on the energetic and statistical mechanical origins of undesirable nonspecific adsorption of synthetic biopolymers in cellular environments are discussed. © *2006 American Institute of Physics*. [DOI: 10.1063/1.2359437]

I. INTRODUCTION

The study of statistical mechanics of polymer adsorption on surfaces is of central importance to many chemical and biological processes as well as a broad spectrum of technological applications. Notably, combinatorial directed evolution techniques have been used to create *de novo* designed peptide sequences that bind specifically to solid surfaces.[1] In general, the proximity of a polymer to a surface can induce significant conformational changes. These include the formation of enhanced amounts of helix- and sheet-like motifs similar to protein secondary structures.[2] Homopolymer adsorption theories have been relatively well studied (see De'Bell and Lookman[3] for a review). Many recent theoretical[4] and computational[5] advances have also been made in the study of copolymer adsorption. For instance, Issaevitch *et al.*[6] applied a Gaussian chain model of copolymers to study the adsorption onto regularly patterned surfaces, and Genzer[7] devised a three-dimensional self-consistent field model to study adsorption of copolymers from a copolymer/homopolymer mixture onto random surfaces. In this context, adsorption of block copolymers is of special interest to numerous experimental[8,9] and theoretical[10,11] investigations (see Alexandridis and Holzwarth[12] and Bates and Fredrickson[13] for reviews) owing to its diverse applications in colloidal stabilization,[14] protein immobilization,[15,16] nanopattern formation,[17–19] and pattern recognition.[20–23]

"Pattern recognition" in copolymer (macromolecule) adsorption refers to the adjustments of the conformations of macromolecules to optimize their interactions with the chemical patterns on surfaces. Naturally, in the presence of a surface with attractive and repulsive sites, a copolymer tends to touch the surface on the attractive sites and avoid the surface at the repulsive sites. There is considerable effort to design and synthesize patterned surfaces and macromolecules that can recognize them.[19,24–26] Biological adsorption *in vivo* appears naturally well designed. Proteins, polysaccharides, and other biomolecules present precisely structured ensembles of organic functional groups to trigger highly specific responses. Synthetic materials used in medical devices such as implants, however, often elicit nonspecific responses when placed in living systems: Instead of specific adsorption, multiple types of proteins, from a mixture of 200 or more types of proteins that comprise most biological fluids, are typically adsorbed onto a synthetic material. Thus, developing an ability to better understand the process of adsorbing proteins and cells on surfaces[27] is important in many areas of research including biosensor technology[17] and tissue engineering.[19] For example, by placing receptor sites onto the materials used in medical applications and biomedical investigations, cell and tissue reactions to those materials might be accurately controlled.[18]

To gain insights into the main determining factors of pattern recognition, here we study a simple self-avoiding lattice block copolymer interacting with a patterned surface. To explore a range of possible applications, predictions from three models with different forms of copolymer-surface interactions are investigated.

[a]Author to whom correspondence should be addressed. Mailing address: Department of Biochemistry, University of Toronto, Medical Sciences Building, 1 King's College Circle, Toronto, Ontario M5S 1A8, Canada. Fax: +1 416 978 8548; Electronic mail: msabaye@arrhenius.med.toronto.edu

II. MODELS

The copolymers are made of alternating blocks of A and B monomers, and the patterned surfaces consist of C and D patches. In model I, A monomers interact with C sites on the surface via an attractive energy, whereas all other interactions (A-B, A-D, B-C, and B-D) are neutral, i.e., have zero energy. A certain degree of pattern recognition behavior is expected for model I as A monomers would tend to be adsorbed onto C sites. This interaction scheme may be considered as the most basic. To study the effect of enhanced specificity on the adsorption transition, we consider also model II, in which A monomers interact favorably with C sites and B monomers interact favorably with D sites (interactions are neutral otherwise). For model II, different parts of the copolymers are attracted to different parts of the patterned surface; so if conditions are favorable, we expect essentially the entire copolymer to lie on the surface forming a specific pattern. In model III, A monomers interact via an attractive energy with C sites but B monomers interact via a repulsive energy with D sites (interactions are neutral otherwise). This construct is designed to explore how pattern recognition specificity may be enhanced by the introduction of repulsive copolymer-surface interactions. In this case, we expect that both adsorbed and desorbed regions to be present. We compare the sharpness of the adsorption transitions and the patterns formed by these three models to gain insights into the role played by interaction specificity in the recognition process and pattern formation. As the aim of this work is to understand pattern recognition in the context of adsorption of copolymers, we have not included self-interactions within the copolymer chain (aside from the self-avoiding excluded volume constraint, i.e., A-A, B-B, and A-B contact interactions are always neutral). This modeling assumption is designed to isolate the adsorption process. Once the adsorption is better characterized, the present models can be augmented with copolymer self-interactions to examine the interplay between chain collapse[2] and pattern-recognizing adsorption.

III. COMPUTATIONAL METHODS

We model block copolymers as n-vertex self-avoiding walks (with $n-1$ edges) on the simple cubic lattice Z^3. The vertices of the walk are numbered $i=1,2,\ldots,n$, with each vertex corresponding to a monomer. We assign the first block of L vertices to be A monomers, the next block of L vertices to be B monomers, and so on, with alternating blocks of A and B monomers of length L. The adsorbing surface consists of the entire $z=0$ plane. Thus, owing to excluded volume, the copolymer is restricted to one side of the adsorbing surface. Without loss of generality, we constrain all monomer positions of the copolymer to $z>0$. The sites on the surface are divided into alternating square blocks of C and D sites. The surface blocks have dimensions $l\times l$. Unless stated otherwise, we use $l=L=5$ in the present study. The model copolymer is tethered to the surface, with the first monomer fixed at position (0,0,1). The origin (0,0,0) corresponds to a corner of a C block (Fig. 1). Using a tethered chain will allow for the possibility of obtaining results for a grafted copolymer which has many interesting applications and provides a systematic

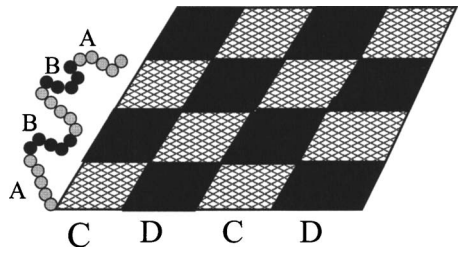

FIG. 1. Schematics of the interaction between a block copolymer and a patterned adsorbing surface.

progress from previous studies of copolymers interacting with homogeneous surfaces[5] to those interacting with patterned surfaces. The copolymer-surface interaction strength may be expressed in units of $\alpha\equiv-\epsilon/k_BT$, where ϵ is a nearest-neighbor contact energy and k_BT is Boltzmann constant times absolute temperature. Interactions are attractive (favorable) if $\epsilon<0(\alpha>0)$ and repulsive (unfavorable) if $\epsilon>0(\alpha<0)$.

We generate a correlated sample of walks using a Metropolis sampling scheme, with the trial moves proposed by a pivot algorithm[28] coupled with local moves. To speed up convergence we use a multiple Markov chain scheme[29] in which we run a set of Markov chains in parallel at different values of α with swapping of configurations between adjacent values of α. In a typical multiple Markov chain simulation, one samples at a variety of different temperatures at the same time and "swaps" configurations between different temperatures with swap probabilities chosen so that the converged distribution of the process is the product of the Boltzmann distributions at the individual temperatures. This method requires that convergence should be rapid at one of the α values, and we achieve this by always including $\alpha=0$ in the multiple Markov chain runs. For details see Geyer[29] and Tesi *et al.*[30]

In model I, we examine the adsorption behavior of a block copolymer whose A monomers interact with only the C sites on the surface. Let $c_n(v_{AC})$ be the number of n-monomer conformations with v_{AC} A-C contacts (v_{AC} is the number of A monomers positioned next to a C site). The partition function for this model is

$$Z_n(\alpha)=\sum_{v_{AC}} c_n(v_{AC})e^{\alpha v_{AC}}. \tag{1}$$

Thus, the free energy $\kappa_n(\alpha)$ per monomer in units of k_BT for an n-monomer copolymer interacting with the adsorbing surface is given by

$$\kappa_n(\alpha)=-n^{-1}\ln Z_n(\alpha). \tag{2}$$

To study the adsorption transition, we compute the average number of A-C contacts, viz.,

$$\langle v_{AC}(\alpha)\rangle=\frac{\Sigma_{v_{AC}} v_{AC}c_n(v_{AC})e^{\alpha v_{AC}}}{\Sigma_{v_{AC}} c_n(v_{AC})e^{\alpha v_{AC}}} \tag{3}$$

as a function of α, where $\langle\cdots\rangle$ denotes Boltzmann averaging over the copolymer conformational ensemble. To allow for comparison on the same footing of the behaviors of copolymers of different chain lengths, we focus on the quantity

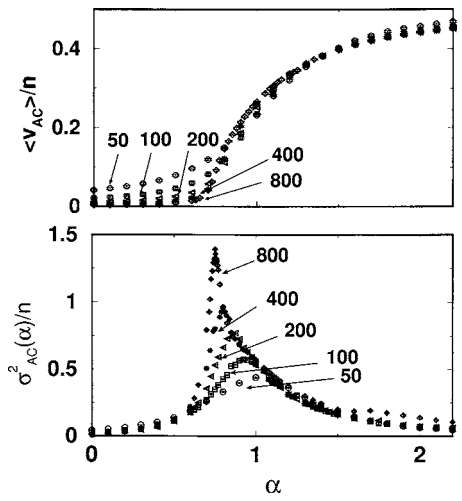

FIG. 2. Average fractional number of A-C contacts (upper panel) and the per-monomer variance $\sigma^2_{AC}(\alpha)/n$ (lower panel) as a function of α for model I. In this and subsequent figures, results for copolymers of different lengths are plotted with different symbols; error bars are determined from block averages; number labels correspond to the number of monomers of the copolymers. Throughout this work, the numbers of simulation steps (one simulation step consists of one pivot move and length divided by four local moves where length is the number of monomers, i.e., vertices of the self-avoiding walk) we have simulated are 1×10^6, 2×10^6, 4×10^6, 8×10^6, and 2×10^7, respectively, for $n=50$, 100, 200, 400, and 800.

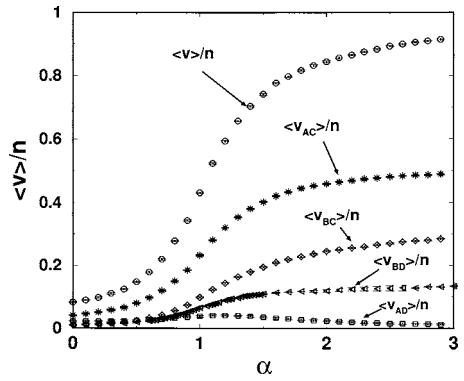

FIG. 3. Average fractional number of various types of copolymer-surface contacts as functions of α for a copolymer with $n=50$ monomers in model I. The top curve $\langle v\rangle/n$ represents the fractional total number of copolymer-surface contacts.

$\langle v_{AC}(\alpha)\rangle/n$, which is normalized by the number of monomers of the copolymer. Formulas for models II and III are defined analogously. The quantity

$$-\frac{\langle v_{AC}\rangle}{n}=\frac{\partial\kappa_n(\alpha)}{\partial\alpha} \tag{4}$$

is related to the energy of the model system [e.g., energy $=\epsilon\langle v_{AC}(\alpha)\rangle$ for model I]. To quantify the sharpness of the adsorption transition, we consider also the fluctuation (or variance) of v_{AC} by computing

$$\frac{\sigma^2_{AC}(\alpha)}{n}=\frac{\langle v^2_{AC}\rangle-\langle v_{AC}\rangle^2}{n}. \tag{5}$$

The quantity $\sigma^2_{AC}(\alpha)/n$ is normalized by the number of monomers of the copolymer and is proportional to the heat capacity, $C(\alpha)$, of the model system (see below). For each of the three models we have investigated, we compute $\langle v_{AC}\rangle$, $\langle v_{AD}\rangle$, $\langle v_{BC}\rangle$, and $\langle v_{BD}\rangle$, for all copolymer-surface contact types and their variances; and in one example, we compute also the root-mean-square distance from the adsorbing surface. The adsorption transition is characterized by monitoring the variation of these thermodynamic and geometric properties over a range of α from zero to values that are far inside the adsorbed regime and for several different chain lengths up to $n=800$ monomers.

IV. RESULTS AND DISCUSSION

A. Model I

The only type of favorable interactions in this model is that between an A monomer and a C site. The mean fraction of A-C contact per monomer is shown in the upper panel of Fig. 2 as a function of α for block copolymer chains of various lengths. For every chain length we studied, $\langle v_{AC}\rangle/n$ undergoes a sigmoidal adsorption transition when the strength of the attractive interaction, α, is sufficiently strong. As α increases, the $\langle v_{AC}\rangle/n$ curves approach an asymptotic value of 0.5 as $\alpha\to\infty$. Because 0.5 is the fraction of A monomers in the copolymer (the chains we study have the same number of A and B blocks), this result means that the A monomers are almost fully adsorbed onto the C surface sites when α is somewhat larger than a transition temperature $\alpha_m(n)$. The sigmoidal transition from desorbed (low level of A-C contacts) to adsorbed (high level of A-C contacts) becomes sharper as chain length n increases. This trend is even more clearly exhibited by the per-monomer variance $\sigma^2_{AC}(\alpha)/n$ of v_{AC} given in the lower panel of Fig. 2. The peak value of $\sigma^2_{AC}(\alpha)/n$ increases with n [we refer to the value of α at which $\sigma^2_{AC}(\alpha)/n$ is maximum as $\alpha_m(n)$], and a lower interaction strength is needed for the adsorption transition with increasing n [i.e., $\alpha_m(n)$ decreases with increasing n]. The peaks in these finite systems exhibit a one-sided shape (being very steep on the small α side of the transition) characteristic of adsorption behaviors.

In this model, the adsorbing behavior of the B monomers is very different from that of the A monomers because the contact interaction of the B monomers with the surface is neutral. To obtain a more detailed picture of possible pattern formation on the surface, Fig. 3 examines the populations of all possible monomer-surface contact types (A-C, A–D, B-C, and B-D, where v_{XY} denotes the number X-Y contacts) as functions of α. The simulated data show that the total fraction, $\langle v\rangle/n$, of adsorbed monomers on the surface asymptotically approaches unity, indicating that the entire copolymer tends to lie on the surface at large α.

Two features in Fig. 3 are noteworthy. First, although the value of $\langle v_{AD}\rangle$ is very low for the entire range of α, the variation of $\langle v_{AD}\rangle$ as a function of α is nonmonotonic. It attains a maximum value of $\alpha\sim1$ in the overall desorbed-adsorbed transition region. This implies that as α increases from an initially low value, A monomers begin to be adsorbed onto C surface sites (sharp increase in $\langle v_{AC}\rangle$). But this process also places some A monomers into contact with D surface sites, even though the A-D interaction is neutral. This leads to a transient increase in A-D contacts until α is suffi-

ciently strong to overcome configurational freedom, such that these D-contacting A monomers can be pulled away toward the C sites. Second, the fraction of B monomers adsorbed onto the D surface sites approaches ≈ 0.12 at high α, which is significantly smaller than the fraction 0.5 of B monomers in the copolymer, and that a relatively larger fraction of B monomers is lying on C surface sites even though they do not have favorable interaction with either C or D sites. Clearly, the reason for the considerable fraction of B monomers lying on the surface is that although the B monomers themselves gain no energetic advantage by sticking onto the surface, they are being "pulled" toward the surface by blocks of "sticky" A monomers. This consideration explains $\langle v_{BC}\rangle > \langle v_{BD}\rangle$ because the A monomers are overwhelmingly stuck to the C sites at high α ($\langle v_{AD}\rangle \approx 0$); so the B monomers that are pulled along tend to be in contact with neighboring C sites. Taken together, the message from Fig. 3 is that whereas the A monomers recognize C surface sites and adsorb accordingly, the B monomers do not stay away from the surface, nor do they stick faithfully to C or D sites. Consequently, a nonuniform pattern is formed on the surface. To ascertain the generality of this behavior, we have repeated the computation for $L=l=10$ and obtained results similar to the $L=l=5$ case here (data not shown). While size factors such as the length of the copolymer blocks control the spacing of the adsorbed blocks in the patterns formed on the surface, the determining factor for the tightness of adsorption is the strength (ϵ contained in α) and the form of the copolymer-surface interaction energy. For model I, the pattern formed by the copolymer on the surface is not orderly and uniform because of the prevalence of nonspecific adsorption. Therefore, if the formation of a more ordered pattern is the objective, the interaction scheme of model I has to be augmented or modified.

B. Model II

We now consider model II. As described above, both A-C and B-D contacts are attractive in this model, with the same interaction strength α. Compared to model I, the interaction scheme of model II is more specific because now the B monomers would prefer contacting the D sites over the C sites on the surface. The variation of $\langle v_{AC}\rangle/n$ for several copolymer chain lengths as functions of α is shown in the upper panel of Fig. 4. As for model I, $\langle v_{AC}\rangle/n$ undergoes a sigmoidal transition and tends to 0.5 when α is increased beyond a transition regime. Essentially identical trends are observed for $\langle v_{BD}\rangle/n$ for the adsorption of B monomers onto D surface sites (data not shown). Clearly, with sufficiently large α, essentially all A and B monomers in this model can find the C and D surface sites, respectively, and adsorb to them. (Hence the equivalence of Fig. 3 of model II would indicate $\langle v_{AD}\rangle/n$, $\langle v_{BC}\rangle/n \to 0$ for large α; data not shown.) The per-monomer variance of contact number $\sigma^2_{AC}(\alpha)/n$ as a function of α is shown in the lower panel of Fig. 4. Compared to model I, the α value at transition, $\alpha_m(n)$, as determined by the location of the maximum of $\sigma^2_{AC}(\alpha)/n$, shifts to much smaller values. (Note that the horizontal scale covers a smaller range of α values in Fig. 4 than that in Fig. 2.) This

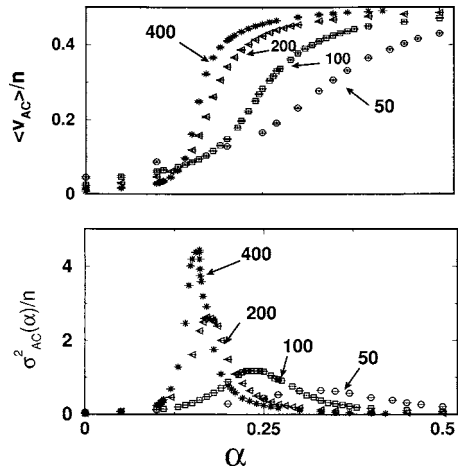

FIG. 4. Same as Fig. 2, but for model II.

is because model II has double the number of possible favorable contacts than model I. As in model I, and as is expected from general considerations of phase transitions, the height as well as the sharpness of the $\sigma^2_{AC}(\alpha)/n$ peak increase with increasing n. At sufficiently large α, because $\langle v_{AC}\rangle/n$, $\langle v_{BD}\rangle/n \to 0.5$ (i.e., $\langle v_{AC}\rangle/n + \langle v_{BD}\rangle/n \to 1$), the adsorbed copolymer lies flat on the surface with alternating blocks of A and B monomers stuck to alternating blocks of C and D surface sites, respectively. Achieving a flat surface pattern of copolymers is important in certain biotechnology applications, as a sticky layer formed as a result of surface adsorption can be useful for preparation of cell seeding.[16]

Kriksin *et al.*[23] have studied a similar model surface adsorption system using a Gaussian model copolymer chain interacting with a surface composed of stripes with different interactions with the copolymer. Interestingly, these authors observed a two-step transition: first a general, not-so-specific adsorption, then a reorganization of the adsorbed copolymer conformation to optimize copolymer-surface interactions. This phenomenon is characterized by two separate peaks in the heat capacity function.[23] We do not observe such a two-stage transition characterized by two separated $\sigma^2_{AC}(\alpha)$ peaks in our models. This difference in transition scenario could be due to a variety of reasons, including the difference in the surface pattern (chess board versus stripes), lattice versus continuum chain representations, the presence of repulsive interactions in the model of Kriksin *et al.*,[23] and differences in adsorption energetics for chains attached to the surface versus that for chains not restricted by a tether constraint.[2] Nonetheless, the nonmonotonic variation of $\langle v_{AD}\rangle$ with α in Fig. 3 for model I (see above) does suggest that a certain degree of optimization and reorganization occurs after adsorption in our model I. It would be instructive to explore these questions in future studies.

C. Model III

To explore the impact of repulsive interactions in pattern recognition, we now consider, as a first step, an interaction scheme with A monomers interacting favorably with C surface sites but B monomers interacting unfavorably with D surface sites. As in protein folding, although repulsive inter-

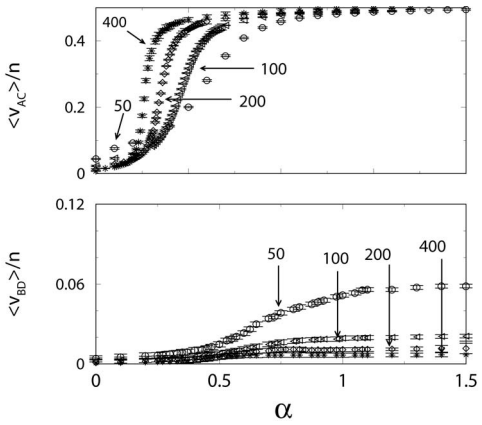

FIG. 5. Average fractional number of *A-C* (upper panel) and *B-D* (lower panel) contacts as functions of α for copolymers of various chain lengths (as indicated by labels for n values) in model III.

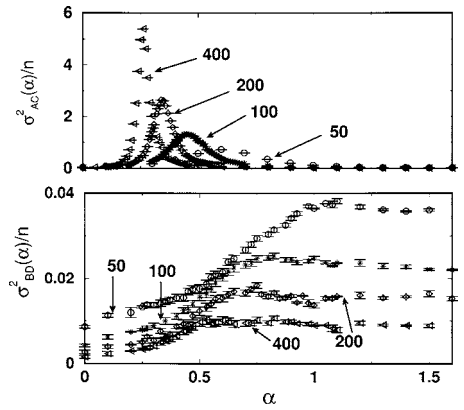

FIG. 6. Per-monomer variance of *A-C* contacts [$\sigma^2_{AC}(\alpha)/n$, upper panel] and per-monomer variance of *B-D* contacts [$\sigma^2_{BD}(\alpha)/n$, lower panel] for various chain lengths (as indicated by labels for n values) as functions of α for model III.

actions are not necessarily present in ground-state configurations, they can be important in lowering the population of undesirable excited-state configurations and thus resulting in a sharper order-disorder transition. This role of repulsive interactions is sometimes referred to as "negative design," in contrast to the role of "positive design" played by the attractive interactions.[31,32] Here, the *A-C* contact interaction strength is parametrized by $\alpha>0$ as in models I and II, whereas the *B-D* contact interaction is repulsive with an interaction strength given by $\gamma<0$. The value of γ is kept constant independent of variations in α. We refer to this construct as model III, which may be viewed as a possible simplified model for surface-induced nanopattern formation in ultrathin films of block copolymers.[27] Physically, the model III interaction scheme means that the population, or Boltzmann weight, of *B-D* contacts is not affected by external conditions that modulate the Boltzmann weight of *A-C* contacts.[33] We use $\gamma=-0.3$ in the present study. Obviously, other forms of repulsive interactions in pattern recognition are possible.[23] In order to assess the robustness of simple-model predictions,[32] an extensive set of physically plausible interaction schemes remains to be investigated.

Figure 5 shows $\langle v_{AC}\rangle/n$ (upper panel) and $\langle v_{BD}\rangle/n$ (lower panel) as functions of α. The average fractional number of the attractive *A-C* contacts $\langle v_{AC}\rangle/n$ tends toward 0.5 as α increases. As for models I and II, the transition becomes sharper as the chain length of the copolymer increases. Notably, even though model I and III have the same favorable *A-C* interactions, the transition midpoints $\alpha_m(n)$ of model III chains shift to lower values than that of corresponding model I chains with the same length. The *A-C* adsorbed state now requires a smaller α value to achieve. In other words, the presence of the *B-D* repulsive interactions makes the adsorbed state more stable. This is consistent with observations from heteropolymer models of protein folding. In those cases, the introduction of repulsive interactions for undesired (nonnative) interactions can raise the stability of the ground state by a negative design mechanism of destabilizing intermediate conformations, even though the repulsive interactions do not affect the ground-state structure.[34]

Not surprisingly, since *B-D* interactions are repulsive, $\langle v_{BD}\rangle/n$ remains at a low level for all α. Broadly speaking, and as expected, the *A* monomers tend to stick to the *C* surface sites whereas the *B* monomers tend to avoid the *D* surface sites. Nonetheless, it is noteworthy that the average fractional number of *B-D* contacts exhibits an increase as $\langle v_{AC}\rangle/n$ undergoes a sharp adsorption transition. This increase in unfavorable interactions, reminiscent of phenomena described by the "frustration" concept in other areas of condensed matter physics,[35,36] is likely caused by the "pulling" effect of the favorable *A-C* contacts, similar to the increase in neutral interactions discussed above for the other two models. Interestingly, this effect diminishes with increasing copolymer chain lengths, at least for the range of α we studied. Apparently, longer chain lengths allow for more configurational possibilities such that unfavorable *B-D* interactions can be avoided more effectively.

Figure 6 compares the fluctuation $\sigma^2_{AC}(\alpha)/n$ in the fractional number of *A-C* contacts (upper panel) against the fluctuation $\sigma^2_{BD}(\alpha)/n$ in the fractional number of *B-D* contacts (lower panel). Every $\sigma^2_{AC}(\alpha)/n$ function exhibits a single peak. As for models I and II, and was evident from the upper panel of Fig. 5, the sharpness of the transition as monitored by *A-C* contacts increases with increasing copolymer chain length. In contrast, whereas $\sigma^2_{BD}(\alpha)/n$ undergoes an increase in the transition region, the fluctuation does not subside sharply as α increases further. This behavior is very different from that of $\sigma^2_{AC}(\alpha)/n$. The $\sigma^2_{BD}(\alpha)/n$ peaks are significantly suppressed in height by approximately two orders of magnitude relative to that of $\sigma^2_{AC}(\alpha)/n$. The increase in fluctuation $\sigma^2_{BD}(\alpha)/n$ (lower panel of Fig. 6) at $\alpha\sim0.75$ appears to coincide and correlate with an increase in the fractional number of *B-D* contacts (lower panel of Fig. 5), most likely because of the pulling effect discussed above. Opposite in trend to that of $\sigma^2_{AC}(\alpha)/n$, the lower panel of Fig. 6 shows that the maximum value of $\sigma^2_{BD}(\alpha)/n$ decreases with increasing copolymer chain length n. These data indicate that, for model III, the copolymer conformations formed near the adsorbing surface at not-so-high α likely consist of alternating blocks of adsorbed *A* monomers and partially desorbed blocks (loops) of *B* monomers (see below).

The sharpness of the adsorption transition is also re-

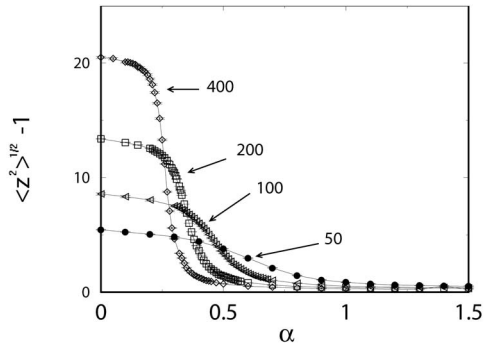

FIG. 7. The root mean square, $\langle z^2\rangle^{1/2}$, of the z coordinates of each of the copolymers of various lengths (as indicated by labels for n values) undergoes an adsorption transition as α increases. Data for model III are shown as an example. The minimum possible $z-1$ value in the model is zero. The quantity $\langle z^2\rangle^{1/2}-1$ is plotted here to highlight its asymptotic approach to zero as α increases.

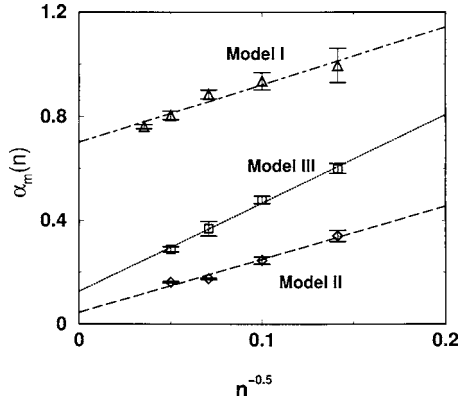

FIG. 9. The location $\alpha_m(n)$ of $\sigma^2_{AC}(\alpha)/n$ peaks vs $1/\sqrt{n}$ for the three models: I ($\triangle$), II ($\diamond$), and III ($\square$). The lines are least-squares fits to the simulation data. Error bars are given by the two simulated α values sandwiching α_m.

flected in the variation of the root-mean-square z coordinate of the copolymer as a function of α (Fig. 7). The quantity $\langle z^2\rangle^{1/2}$ measures the average distance of the copolymer from the $z=0$ adsorbing surface. The minimum possible value of z is unity and therefore the minimum possible value for $z-1$ is zero. Comparing Fig. 7 with Figs. 5 and 6 shows that the point $\alpha_m(n)$ of v_{AC}/n transition corresponds essentially also to the point of a "flattening" transition (rapid decrease in root-mean-square z value of the copolymer). The plotted data show that for α significantly larger than α_m, the copolymer tends to lie flat on the surface $[(\langle z^2\rangle^{1/2}-1)\to 0]$. This is because the repulsive interaction in model III is independent of α. Thus, at sufficiently large α, the repulsive B-D interactions are overwhelmed by the attractive A-C interactions.

Figure 8 shows the average fractional contact number for all four types of copolymer-surface contacts. A large fraction of B monomers is sticking to C surface sites, likely because of pulling effects of the favorable A-C interactions, as in Fig. 3 for model I. However, pattern recognition is more specific in model III than in model I because of the presence of the repulsive B-D interactions. As a result, $\langle v_{BD}\rangle/n$ is significantly lower than that for model I. Interestingly, $\langle v_{BD}\rangle/n \approx \langle v_{AD}\rangle/n$, and the fractional number of favorable A-C contacts in model III is somewhat lower than that in model I, but the fractional number of neutral A-D contacts in model III is

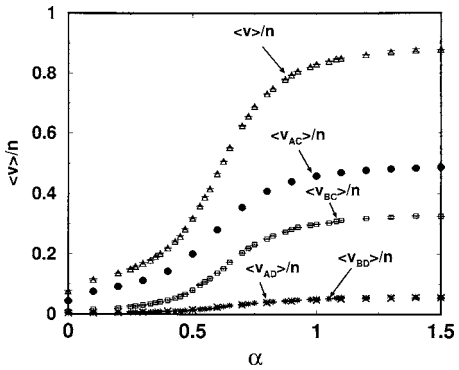

FIG. 8. Average fractional number of various types of copolymer-surface contacts as functions of α for a copolymer with $n=50$ in model III. (Same as Fig. 3 but now for model III.)

higher than that in model I. This phenomenon originates from the repulsive B-D interactions. To avoid these unfavorable contacts as much as possible (as they cannot be avoided altogether in the model), some favorable A-C contacts have to be sacrificed. Apparently, an overall consequence of the B-D repulsion is that the copolymer does not lie as flat on the surface; the average fractional total number of copolymer-surface contact $\langle v\rangle/n$ is somewhat lower in model III than in model I. These model observations highlight the possible subtle effects that can be achieved through an interplay of attractive and repulsive interactions. One of the issues that synthetic biopolymers in the cell encounter is nonspecific adsorption which triggers undesirable events and leads to possibly harmful physiological pathways.[18] As repulsive interaction can enhance specificity, using them extensively in design can in principle lead to more specific adsorption pattern, and interfaces with more versatile adhesive properties, e.g., with some chain segments extend from the surface.

D. $n\to\infty$ asymptotic behavior

Comparison of the σ^2_{AC}/n plots in Figs. 2, 4, and 6 indicates that for every chain length n we have studied, the $\alpha_m(n)$ transition points (at peak σ^2_{AC}/n) of the three models follow the order $\alpha_m(\text{model I})>\alpha_m(\text{model III})>\alpha_m(\text{model II})$. A general method to study the trend of phase transition behavior has been to plot $\alpha_m(n)$ of finite systems versus $n^{-\phi}$, where ϕ is a crossover exponent that controls the way in which the peak positions $\alpha_m(n)$ asymptotically approach the critical point α_c of adsorption for the corresponding infinite-size system $[\alpha_c=\lim_{n\to\infty}\alpha_m(n)]$. For homopolymer adsorption, numerical estimates of ϕ range from ~0.5 to 0.59 (De'Bell and Lookman[3]). Here, the number of data points computed for the three models is not sufficient for an independent estimate of ϕ. To make progress, we assume $\phi=0.5$ as in models of adsorption of homopolymers and periodic copolymers. Figure 9 shows that for $n>100$, there is a reasonably linear relationship between the simulated $\alpha_m(n)$ values and $n^{-1/2}$ for our models. Based on the assumption that this linear dependence may be extrapolated to $n^{-1/2}\to 0$ (i.e., $n\to\infty$), the rough estimates for α_c we obtain for models I, II, and III are, respectively, ≈0.70,

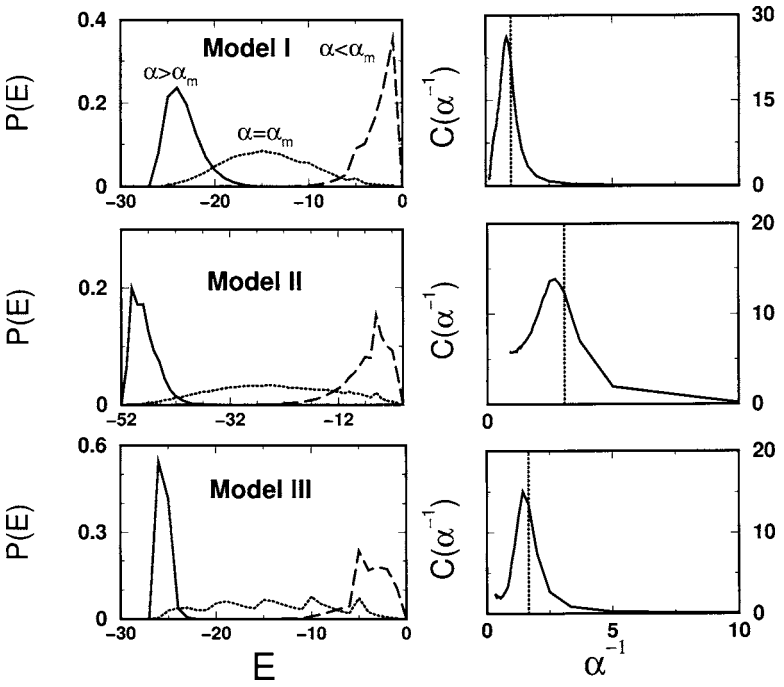

FIG. 10. Potential energy distributions (left panels) and heat capacities (right panels) for the three models in this work ($n=50$). For every model, the energy distribution is provided for three different α values that are significantly greater than, equal to, and significantly less than α_m (plotted as solid, dotted, and dashed curves, respectively). These α values in the left panels are 2.0, 1.0, and 0.2 for model I, 1.0, 0.33, and 0.1 for model II, and 2.5, 0.6, and 0.1 for model III. The dotted vertical lines in the heat capacity plots (right panels) mark the α_m^{-1} values at the corresponding σ_{AC}^2/n peaks. They are slightly offset from the peak heat capacity values because the heat capacity accounts for all interaction energy instead of only the *A-C* contacts and it also contains a factor of T^{-2} that is absent in σ_{AC}^2/n.

0.045, and 0.14. Consistent with the trend noted above for finite-size systems, Fig. 9 shows that merely incorporating repulsive interactions without adding attractive interactions can lead to a decrease of α_c for model III relative to that of model I. But a more substantial decrease in α_c results from the additional attractive interactions in model II that are not present in model I.

E. Energy distribution and calorimetric measurements

To better understand the energetic basis of adsorption transitions and to explore novel experimental avenues to investigate them, we now consider the potential energy distributions (referred to below simply as energy distributions) of our three model systems and their temperature dependence. The main motivation here is to ascertain the implications of different adsorption scenarios on possible measurements using scanning calorimetry, an experimental technique that has been used extensively to characterize order-disorder transitions such as the folding/unfolding transitions of proteins.[37–40]

Treating the model parameter ϵ as a constant, the total copolymer-surface interaction energy E, in units of $|\epsilon|$, is $E=-v_{AC}$ for models I and III (note that γ which quantifies the *B-D* interactions is a constant), and $E=-v_{AC}-v_{BD}$ for model II. Accordingly, the absolute temperature $T=\alpha^{-1}$ in units of $|\epsilon|/k_B$. By definition, the (constant-volume) heat capacity

$$C(T)=\frac{d\langle E\rangle}{dT}=\frac{\langle E^2\rangle-\langle E\rangle^2}{k_BT^2} \tag{6}$$

is the energy variance divided by k_BT^2. Thus, the heat capacity in units of k_B, $C(\alpha^{-1})/k_B=\alpha^2\sigma_{AC}^2$ for models I and III, and $C(\alpha^{-1})/k_B=\alpha^2[\sigma_{AC}^2+\sigma_{BD}^2+2\langle v_{AC}v_{BD}\rangle-\langle v_{AC}\rangle\langle v_{BD}\rangle]$ for model II. As there is no risk of confusion, below we will refer to $C(\alpha^{-1})/k_B$ simply as $C(\alpha^{-1})$.

For each of the three models, the left panels of Fig. 10 show the energy distributions [$P(E)$ for $n=50$] at a low temperature (small α^{-1}) when the copolymer is adsorbed, around the adsorbed/desorbed transition temperature [$\approx\alpha_m(n)^{-1}$], and at a high temperature (large α^{-1}) when the copolymer is desorbed. If the adsorption transition is "first-order-like" (i.e., "two state" or "all or none" in the terminology of certain biomolecular transitions[38,40]), the energy distribution at transition, α_m, would be bimodal, exhibiting two peaks simultaneously at essentially the same positions as the peaks of the energy distribution, respectively, at low temperature ($\alpha\gg\alpha_m$) and high temperature ($\alpha\ll\alpha_m$).[40] Figure 10 shows that none of the three models satisfies this condition, as their energy distributions at transition are all unimodal although they are more spread out. The fact that energy distribution is spread out at transition is consistent with the diverging trends in σ^2/n plots for the three models in Fig. 2 (lower panel), Fig. 4 (lower panel), and Fig. 6 (upper panel). It is interesting to note that the transition energy distributions for models II and III are more spread out than that of model I; the detailed mechanism by which enhanced interaction specificity can move the behavior of the adsorption transition toward acquiring characteristics akin to that of a two-state-like transition requires further study.

In scanning calorimetry experiments, the calorimetric enthalpy $\Delta H_{\rm cal}$ is the total heat absorbed by the system to effect an ordered to disordered transition:

$$\Delta H_{\rm cal}=\int dTC_P(T), \tag{7}$$

where $C_P(T)$ is temperature-dependent, constant-pressure heat capacity, and the integration is over the transition region with appropriate base line subtractions.[37,39] Here, the energy in Eq. (6) may be identified with experimental enthalpy when pressure-volume effects are negligible, as for many applications under ambient conditions. Hence, $C(T)$ in Eq. (6) may be identified with $C_P(T)$ and we obtain model equivalence of $\Delta H_{\rm cal}$ by computing area under the $C(\alpha^{-1})$

curves on the right column of Fig. 10. Following the κ_2 definition of Kaya and Chan,[39] the van't Hoff enthalpy

$$\Delta H_{\mathrm{vH}} = 2T_{\max}\sqrt{k_B C(T_{\max})} = 2\alpha_{\max}^{-1}\sqrt{C(\alpha_{\max}^{-1})}, \tag{8}$$

where $T_{\max}=\alpha_{\max}^{-1}$ is the temperature at which the heat capacity function $C(\alpha^{-1})$ attains its maximum value. Thus, ΔH_{vH} is deduced from the same heat capacity plots. Both ΔH_{vH} and ΔH_{cal} are expressed here in units of $|\epsilon|$.

Calorimetric measurements are a useful probe of the underlying energetics because $\Delta H_{\mathrm{vH}}/\Delta H_{\mathrm{cal}}\approx 1$ implies that the order-disorder transition is two-state-like[37,40] for a system that can be essentially completely disordered at sufficiently high temperatures.[38] Since the $P(E)$'s in the left column of Fig. 10 have indicated that our models are not two-state-like, $\Delta H_{\mathrm{vH}}/\Delta H_{\mathrm{cal}}$ is expected to be significantly less than unity.[41] As an illustration, we have determined the van't Hoff to calorimetric enthalpy ratio, $\Delta H_{\mathrm{vH}}/\Delta H_{\mathrm{cal}}$, for model I, for which $C(T)$ values at sufficiently low temperatures are available. To determine ΔH_{cal}, the integration in Eq. (7) was carried out from the lowest to the highest $T=\alpha^{-1}$ values we had simulated. Consistent with expectation, we obtain $\Delta H_{\mathrm{vH}}\approx 8.5$ and $\Delta H_{\mathrm{cal}}\approx 23.3$ and thus $\Delta H_{\mathrm{vH}}/\Delta H_{\mathrm{cal}}\approx 0.36<1$ for model I. The observation that all three of our model interaction schemes do not lead to two-state-like adsorption transitions is reminiscent of recent findings in protein folding that pairwise additive interactions are often insufficient for two-state-like behaviors,[38] and that many-body effects beyond pairwise additivity are likely required for calorimetric two-state cooperativity.[40]

V. CONCLUDING REMARKS

We have used extensive multiple Markov chain Monte Carlo simulations to study possible scenarios of copolymer adsorption on a patterned surface by comparing three different yet related model interaction schemes. Building on a basic copolymer adsorption model (model I), we explored two means of enhancing interaction specificity: the addition of favorable, attractive interactions for desirable copolymer-surface contacts (model II), or the addition of unfavorable, repulsive interactions for undesirable copolymer-surface contacts (model III). Enhanced interaction specificity leads to a sharper adsorption transition, a thermodynamically more stable adsorbed state, and a more uniform pattern formed by the adsorbed copolymer conformation. It is noteworthy that neutral or unfavorable copolymer-surface interactions persist even after the main adsorption transition in all three models, indicating that a level of energetic frustration may not be straightforward to avoid because of chain connectivity constraints. Ultimately, these general principles emerging from simple-model simulations should be useful for practical engineering designs.

In all three models studied, the adsorption transition is not first-order-like: their underlying energy distributions at transition are unimodal, rather than bimodal. In principle, this aspect of the adsorption transition may be experimentally accessible by calorimetry. Previous findings suggest that a sharply cooperative first-order-like adsorption transition would likely require many-body interactions[40] beyond the types of pairwise additive interactions modeled in the present study. The manner in which these many-body interactions will play a significant role in the adsorption problem is open to future investigations.

ACKNOWLEDGMENTS

Helpful discussions with Professor S. G. Whittington are greatly appreciated. Financial support for our research has been provided in part by the Canadian Institutes of Health Research [CIHR Grant No. MOP-15323 to one of the authors (H.S.C.)] Protein Engineering Network of Centres of Excellence (PENCE), and the Canada Research Chairs Program.

[1] J. J. Gray, Curr. Opin. Struct. Biol. **14**, 110 (2004).
[2] H. S. Chan, M. R. Wattenbarger, D. F. Evans, V. A. Bloomfield, and K. A. Dill, J. Chem. Phys. **94**, 8524 (1991); **96**, 3361(E) (1992).
[3] K. De'Bell and T. Lookman, Rev. Mod. Phys. **65**, 87 (1993).
[4] S. G. Whittington, J. Phys. A **31**, 3769 (1998).
[5] M. S. Moghaddam, T. Vrbova, and S. G. Whittington, J. Phys. A **33**, 4573 (2000).
[6] T. A. Issaevitch, D. Jasnow, and A. C. Balazs, J. Chem. Phys. **99**, 8244 (1993).
[7] J. Genzer, J. Chem. Phys. **115**, 4873 (2001).
[8] P. C. Griffiths, T. Cosgrove, J. Shar, S. M. King, G.-E. Yu, C. Booth, and M. Malmsten, Langmuir **14**, 1779 (1998).
[9] S. J. Mears, T. Cosgrove, L. Thompson, and I. Howell, Langmuir **14**, 997 (1998).
[10] J. U. Sommer and M. Daoud, Europhys. Lett. **32**, 407 (1995).
[11] A. Jayaraman, C. K. Hall, and J. Genzer, J. Chem. Phys. **123**, 124702 (2005).
[12] P. Alexandridis and J. F. Holzwarth, Curr. Opin. Colloid Interface Sci. **5**, 312 (2000).
[13] F. S. Bates and G. H. Fredrickson, Annu. Rev. Phys. Chem. **41**, 525 (1990).
[14] D. H. Everett, Chem. Ind., 849 (1977).
[15] T. Ikawa, F. Hoshino, T. Matsuyama, H. Takahashi, and O. Watanabe, Langmuir **22**, 2747 (2006).
[16] E. Brynda, J. Pachernik, M. Houska, Z. Pientka, and P. Dvorak, Langmuir **21**, 7877 (2005).
[17] M. Mrksich and G. M. Whitesides, Trends Biotechnol. **13**, 228 (1995).
[18] B. D. Ratner, J. Mol. Recognit. **9**, 617 (1996).
[19] M. V. Merritt, M. Mrksich, and G. M. Whitesides, *Principles of Tissue Engineering* (Landes, Austin, TX, 1997), p. 211.
[20] M. Muthukumar, J. Chem. Phys. **103**, 4723 (1995).
[21] D. Bratko, A. K. Charaborty, and E. I. Shakhnovich, Chem. Phys. Lett. **280**, 46 (1997).
[22] A. J. Golumbfskie, V. S. Pande, and A. K. Chakraborty, Proc. Natl. Acad. Sci. U.S.A. **96**, 11707 (1999).
[23] Y. A. Kriksin, P. G. Khalatur, and A. R. Khokhlov, J. Chem. Phys. **122**, 114703 (2005).
[24] J. Genzer, Phys. Rev. E **63**, 022601 (2001).
[25] R. S. Kane, S. Takayama, E. Ostuni, D. E. Ingber, and G. M. Whitesides, Biomaterials **20**, 2363 (1999).
[26] A. Jayaraman, C. K. Hall, and J. Genzer, Phys. Rev. Lett. **94**, 078103 (2005).
[27] J. P. Spatz, P. Eibeck, S. Mössmer, M. Möller, E. Yu. Kramarenko, P. G. Khalatur, I. I. Potemkin, A. R. Khokhlov, R. G. Winkler, and P. Reineker, Macromolecules **33**, 150 (2000).
[28] M. Lal, Mol. Phys. **17**, 57 (1969).
[29] C. J. Geyer, in *Proceedings of the 23rd Symposium on the Interface*, edited by E. M. Keramidis (Interface Foundation, Fairfax Station, VA, 1991), p. 156.
[30] M. C. Tesi, E. J. van Rensburg, E. Orlandini, and S. G. Whittington, J. Stat. Phys. **82**, 155 (1996).
[31] H. S. Chan and K. A. Dill, Proteins **24**, 335 (1996).
[32] R. Wroe, E. Bornberg-Bauer, and H. S. Chan, Biophys. J. **88**, 118 (2005).
[33] This phenomenon can arise in a variety of circumstances. For instance, for adsorption that takes place in solution, the copolymer-surface interactions are solvent mediated. Certain chemical reagent such as denatur-

ants and osmolytes may affect the *A*-*C* interaction but not the *B*-*D* interaction. In that case, variation of α may be considered as a model for variation of the concentration of such chemical reagents and this variation would then have no effect on γ. Alternately, if the energy ϵ is kept constant, the variation in α is proportional to the variation in inverse absolute temperature, $1/T$. In this case, then, the constancy of γ may be interpreted as a modeling assumption that the solvent-mediated *B*-*C* interaction is purely entropic in origin (arising from solvent ordering, for example). We use this assumption in the subsequent analysis of heat capacity in the text.

[34] See, e.g., Fig. 1 of H. Kaya and H. S. Chan, Phys. Rev. Lett. **90**, 258104 (2003).
[35] G. Toulouse, Commun. Phys. (London) **2**, 115 (1977).
[36] J. D. Bryngelson and P. G. Wolynes, Proc. Natl. Acad. Sci. U.S.A. **84**, 7524 (1987).
[37] P. L. Privalov and N. N. Khechinashvili, J. Mol. Biol. **86**, 665 (1974).
[38] H. S. Chan, Proteins **40**, 543 (2000).
[39] H. Kaya and H. S. Chan, Proteins **40**, 637 (2000); **43**, 523(E) (2001).
[40] H. S. Chan, S. Shimizu, and H. Kaya, Methods Enzymol. **380**, 350 (2004).
[41] M. Knott and H. S. Chan, Proteins **65**, 373 (2006).